*Available online at* **www.joac.info**

ISSN: 2278-1862

*Journal of Applicable Chemistry*

2019, 8 (2): 884-891

(International Peer Reviewed Journal)

# Morphology and Size Controlled Synthesis of Mixed Valent Ceria Nanostructures

**Sovan Chakraborti[1], Sunanda Dey[2] and Soumitra Kar[3]***

1. ICARE School of Research and Development, Haldia–721657, **INDIA**
2. Department of Chemical Eng., Haldia Institute of Technology, Haldia–721657, **INDIA**
3. Department of Applied Science, Haldia Institute of Technology, Haldi –721657, **INDIA**

Email: kar_mitra@yahoo.co.in

**Accepted on 21st March, 2019**

## ABSTRACT

*We report a simple room temperature based aqueous route to synthesize nearly monodispersed ultra-small (~3 nm) ceria nanoparticles (NP). Ceria NPs were also synthesized by using NaOH assisted hydrothermal routes. Ceria NPs were also synthesized by using ethylenediamine and ethylene glycol as solvent. The results indicated the all the processes produced nearly monodispersed particles. Ethylene glycol assisted route produced smallest (~2.2 nm) particles whereas the room temperature-based process produced water dispersible particles. The ceria NPs possessed a mixed valence state and autocatalytic properties. $Ce^{3+}$ percentage was found to maximum in the room temperature derived sample followed by ethylene glycol derived sample.*

### Graphical Abstract

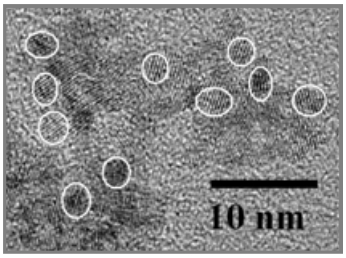


Ceria nanoparticles.

**Keywords:** Ceria, Nanoparticles, Mixed Valency, Oxygen vacancy.

## INTRODUCTION

Cerium oxide (ceria, $CeO_2$) is one of the technologically important rare earth oxide for its unique properties such as oxygen ion conductivity, oxygen storage capacity, high mechanical strength, autocatalytic property and free-radical scavenging property [**1-17**]. Presence of such unique properties make ceria an important material as an oxygen ion conductor in solid oxide fuel cells [**6, 9**] and oxygen sensors [**18**]. Ceria nanoparticles (NPs) are capable of possessing a mixed valence state of Ce

ions (i.e. $Ce^{3+}$ and $Ce^{4+}$ valence state). The ceria NPs are capable of arresting the free radicals that leads to change its oxidation state. Interestingly, ceria NPs are capable of regenerating their reduced ($Ce^{3+}$) valence state form the oxidized ($Ce^{4+}$) valence state thus behaving as a catalyst. This unique property of ceria NPs was utilized to prevent radiation induced cellular damage, retinal degeneration etc [**3, 4, 19, 20**]. Thus, keeping in mind the widespread application of ceria NPs, it is extremely important to explore a simple, inexpensive synthesis strategy for large scale production of ceria NPs. Till date, several methods have been employed to synthesize ceria nanoparticles including flame combustion method [**21, 22**], hydroxide co-precipitation of precursors [**23**], hydrothermal/ solvothermal process [**11, 24, 25**], microemulsion process [**14, 26]** sonochemical and microwave-assisted heating methods [**27**], sol-gel method [**28**] etc [**29-32**].

Ceria NPs synthesized by the above-mentioned methods are often highly aggregated, and large scale synthesis of monodisperse NPs is quite challenging. Only a few organic solvent assisted synthesis routes are reported to produce monodisperse particles [**28**]. It is also important to perform post surface modifications to obtain water-soluble ceria nanoparticles. It is therefore important to develop a robust synthesis method to produce water-dispersible, ultra-small (<5.0 nm) ceria nanoparticles with high yield to meet the growing demand ceria NPs in biomedical applications. In this paper we report a simple, eco-friendly, room temperature aqueous route to produce water-dispersible, ultra-small (~3 nm) ceria NPs. In addition, we have also synthesized nearly monodispersed ceria NPs with different size range by using hydrothermal and solvothermal approaches.

## MATERIALS AND METHODS

Ceria NPs were synthesized by adding 0.434 g $Ce(NO_3)_3.6H_2O$ to a basic solution (0.1 g NaOH dissolved in 32 mL water) followed by 48 h magnetic stirring. The resulting white precipitate was collected and washed several times in water. Ceria NPs remained highly dispersed in DI water for several days studied herein. Ceria NPs are also synthesized by the hydrothermal treatment of the above mentioned reaction mixtures at 100°C and 150°C respectively. For the hydrothermal synthesis the reaction mixture [0.434 g $Ce(NO_3)_3.6H_2O$ and 0.1 g NaOH dissolved in 32 mL water) was transferred to the Teflon lined stainless steel chamber. The closed chamber was then transferred to e preheated oven. Ceria NPs were also synthesized solvothermally at 150°C using ethylenediamine and ethylene glycol as solvents. For the solvothermal synthesis 0.434 g $Ce(NO_3)_3.6H_2O$ was directly added into the desired solvent taken in a Teflon lined stainless steel chamber. For particle characterization using transmission electron microscopy (TEM), the precipitate was re-dispersed in ethanol and deposited on a thin carbon film coated Cu grid. UV-Visible and auto-catalytic activity of ceria NPs were studied using water-dispersed particles. For the X-ray diffraction (XRD) and X-ray photo electron spectroscopic (XPS) studies, vacuum desiccated particles were used. The XRD study was carried out to determine the crystalline phase identity of the products whereas, the XPS study was carried out to determine the chemical composition and valence state of the elements in the ceria nanocrystals.

## RESULTS AND DISCUSSION

The XRD pattern of the dried sample as shown in figure 1 reveals the formation of pure $CeO_2$ with cubic phase (fluorite structure, JCPDS 34-0394, space group *Fm*-3*m*), having lattice constants of 5.414(3), 5.436(3), and 5.405(3) Å, respectively. The broadening of the diffraction pattern could be ascribed to the formation of ceria NPs. Within the limit of the XRD sensitivity, we could not detect the formation of any hydroxide phase [$Ce(OH)_3$]. XRD patterns of the ceria NPs synthesized hydrothermally at 100 and 150$^oC$ are depicted in figure 1b. XRD pattern reveals the formation of relatively larger crystals at the hydrothermal conditions. Figure 1c shows the formation of ceria NPs in ethylenediamine (EN) and ethylene glycol (EG) under the solvothermal treatment at 150 $^oC$. In our earlier work [**11**], we have reported the capping property of EN for the synthesis of ceria NPs. EG is a

well known capping agent for synthesis of various NPs [**33-34**]. Here we have synthesized ceria NPs under the presence of various types of capping agents and the results are compared. The particles sizes of the ceria NPs formed are revealed by the TEM studies and discussed later.

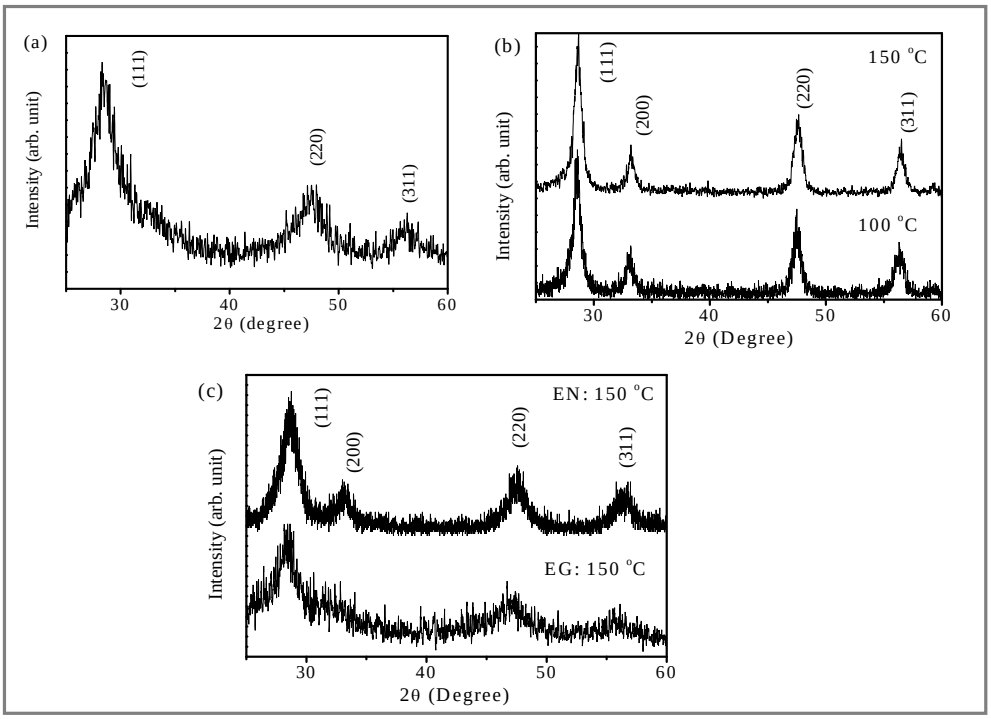


**Figure 1.** XRD pattern of the ceria nanoparticles synthesized at (a) room temperature; (b) hydrothermally in presence of 0.1 g NaOH at 150°C and (c) solvothermally in EN and EG at 150°C.

Morphology and particle size of the ceria NPs were investigated through high resolution TEM (HRTEM). Studies reveal the formation of nearly mono-dispersed ceria NPs with particle size 3.0 ± 0.5 nm. The HRTEM study (image not shown here) clearly demonstrates the formation of single crystalline nanoparticles even at room temperature. Selected area electron diffraction (SAED) pattern recorded on a bunch of ceria nanoparticles exhibits the appearance of bright white rings confirming the formation of crystalline ceria NPs.

Through proper analysis, the rings were indexed to the various crystalline plane of ceria. The results are in good agreement with the XRD pattern. In our synthesis approach, it is important to keep the NaOH concentration low (0.078 M) in order to have a controlled reaction condition allowing proper periodic arrangement of the constituent atoms to form well-faceted nanocrystals. It was observed that the use of high concentration of NaOH (1.56 M and above) triggered rapid and uncontrolled precipitation producing undefined aggregated ceria. Thus, the TEM studies indicated the formation of nearly mono-dispersed ceria NPs at room temperature in presence of a relatively lower concentration of NaOH.

With a view to further understand the formation of mono-dispersed ceria NPs, hydrothermal reactions were carried out at 100 and 150°C respectively. XRD patterns indicated formation of larger particles compared to that obtained at room temperature. Figure 2 show the TEM images of the ceria NPs formed at the hydrothermal conditions. Figures 2a and 2b shows the TEM images of the particles obtained at 100 °C. TEM images show the formation of nearly monodispersed particles with average particle size 9-10 nm. The SAED pattern shown in the inset of figure 2a reveals the formation of $CeO_2$ phase. The HRTEM image in figure 2d indicated the formation of highly crystalline octahedral shape

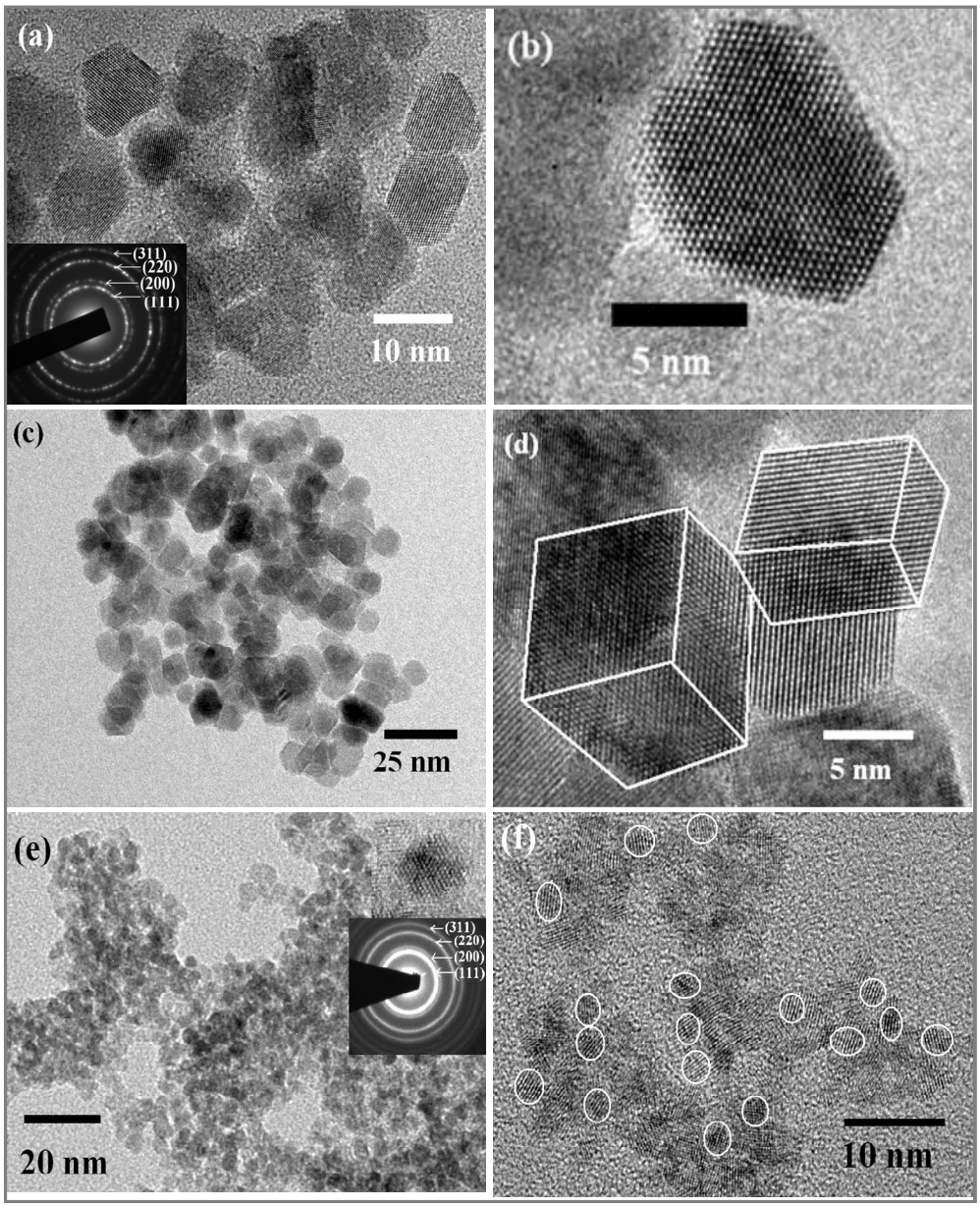


**Figure 2.** TEM images of the particles synthesized hydrothermally at **(a, b)** 100°C, **(c, d)** 150°C and solvothermally at 150°C using**(e)** EN and **(f)** EG.

of the nanoparticles. Figures 2c and 2d show the formation of nearly mono-dispersed cubic shaped ceria NPs at 150°C. The cubic edges of the ceria NPs were marked in the HRTEM image of figure 2d. Evolution of the cubic shape from the octahedral shape at higher temperature could be attributed to formation of stable structures with minimum surface energies at higher temperatures. These results indicated that NaOH when used in appropriate concentrations could act as a size restricting agent for the synthesis of ceria NPs. In order to compare the capping ability of NaOH with other well known capping solvents such as EN and EG, ceria NPs were also synthesized in these solvents under solvothermal condition at 150°C. Figure 2e shows the TEM image of the ceria NPs synthesized using EN at 150°C revealing the formation of nearly monodispersed NPs with average size ~ 4 nm. Inset of the image shows the HRTEM image of one NPs and SAED pattern of the NPs. Figure 2f shows the formation ultra-small (~2.2 nm) particles when EG was used as the solvent for synthesis. These results indicated that EG was the most effective capping solvent to synthesize ultra-small ceria NPs under hydrothermal/solvothermal process. The dispersibility of these particles obtained under various

conditions was tested. It was observed that the NPs obtained at room temperature were dispersible in water.

Based on our experimental findings, we propose the formation mechanism of ultra-small ceria NPs at room temperature as follows. The controlled conversion of solvated cerium ions to ceria NP is mediated by the mild basic environment. Basic reaction condition instantaneously converts cerium hydroxide to ceria nuclei. The mild reaction condition is crucial for promoting controlled nucleation. During the growth process, hydroxide ions are populated to the surface bound cations, providing a unique capping environment. Such environment restricts grain growth by preventing further diffusion of the constituent atoms. The presence of large number of surface hydroxyl groups is responsible for superior aqueous dispersibility of ceria NPs. For biomedical applications, it is highly desirable to obtain water-dispersible high-quality ceria NPs in their mixed valence states.

The particle size distribution and aqueous solubility was also characterized using dynamic light scattering (DLS) technique. The DLS data recorded also indicated the formation of nearly mono-dispersed particles with particle size 6.3 ± 1.0 nm. The appearance of the higher particle size in DLS is compared to the TEM is expected as the DLS provides the hydro-dynamic size of the particle in a solution.

In order to determine the chemical composition and the valence state of the elementary components in the products we have carried out the XPS studies on the powder samples. Figure 3a shows the survey XPS spectrum of the sample synthesized at room temperature demonstrating the presence of Ce and O asthe elementary components. Valence state of the Ce is important in determining the properties and applicability of the ceria NPs. In order to verify the applicability of the ceria NPs it is therefore necessary to investigated in detail the valence state of Ce using high resolution XPS scan in the region of 880-925 eV. The XPS spectrum (Figure 3b) shows the presence of a mixed valence state ($Ce^{3+}$ and $Ce^{4+}$).

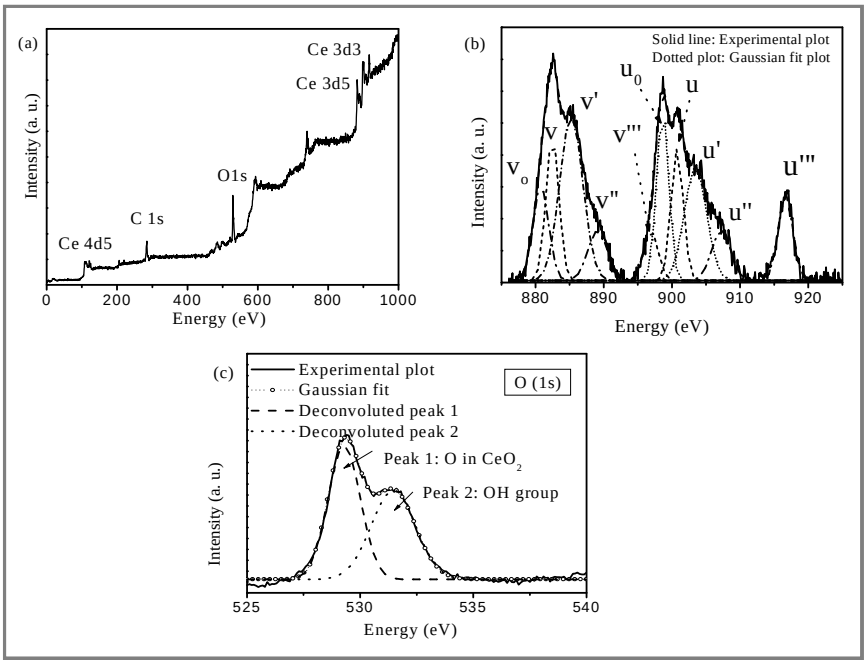


**Figure 3.** XPS spectra of the ceria nanoparticles: **(a)** survey scan and **(b)** high-resolution scan showing the valence states for Ce in the ceria NPs.

The synthesized cerium oxide NPs, the $Ce^{3+}$ ions are introduced in the ceria nanocrystal lattice because of oxygen vacancies of $Ce^{3+}$ ions created by surface chemical reactions. In order to

distinguish the different valence states the spectrum was de-convoluted using Gaussian multi-peak fitting and different peaks were indexed according to the literature [**11, 35**]. In the figure $Ce^{3+}$ state related peaks were attributed as $v_o$, $v'$, $u_o$, and $u'$ and peaks related to $Ce^{4+}$ valence state were depicted as. $v$, $v''$, $v'''$, $u$, $u''$, and $u'''$ respectively. Percentages of the $Ce^{3+}$ compared to that of $Ce^{4+}$ valence states was semi-quantitatively calculated by using the integrated peak area of the respective states as reported on the literature [**11, 35**]

$$[Ce^{3+}]\% = \frac{A_{v_o} + A_{v'} + A_{u_o} + A_{u'}}{A_{v_o} + A_{v'} + A_{u_o} + A_{u'} + A_v + A_{v''} + A_{v'''} + A_u + A_{u''} + A_{u'''}} \times 100\% \quad (1)$$

Nearly 57.1 % of $Ce^{3+}$ was detected in the room temperature derived sample. $Ce^{3+}$ was found to decrease drastically upon hydrothermal treatment and nearly 12 % $Ce^{3+}$ was detected at 150°C. Around 40 and 49 % and $Ce^{3+}$ were detected on the samples solvothermally synthesized using EN and EG respectively. Detail investigation of the high resolution oxygen peak in the XPS spectra (figure 3c) reveals the presence of substantial amounts of OH groups in the sample. However, via cumulative analysis of the data from XRD, HRTEM and SAED patterns, presence of any cerium hydroxide phase in the nanocrystals could be easily ruled out. The presence of hydroxyl groups as determined from XPS must have originated from surface attached hydroxyl groups. NaOH played a critical role as a catalyst for transforming cerium salt to ceria NP and hydroxide ions served as a capping agent to prevent further grain growth.

Since the room temperature derived sample was the only sample dispersible in water, that sample was tested using UV visible spectroscopy for investigating the autocatalytic property. UV-visible transmittance spectra of the sample was recorded in presence and absence of $H_2O_2$ as reported in the literature.[**4, 11, 36**] Digital image of the ceria NP solution in DI water before and after addition of $H_2O_2$ was also recorded. The transparent and colorless ceria NP solution turned reddish brown upon addition of a small dose of $H_2O_2$. The transmittance spectrum of the NPs solution suffered a large red shift upon addition of 10 µl $H_2O_2$. This red-shift in the transmittance spectrum is due to a change in the oxidation state from $Ce^{3+}$ to $Ce^{4+}$ [**17**]. After this measurement, we kept the experimental solution in the dark and UV–visible spectra were recorded for the next 10 consecutive days. A gradual blue shift in the spectra was observed over time. This gradual blue shift reflects the regeneration of the $Ce^{3+}$ oxidation state in the cerium oxide NPs. At the end of the 10 days, the color of the solution faded away and became yellow. When an additional hydrogen peroxide dose was administered to the solution on day 10, the UV–visible spectrum again shifted to lower energy and subsequently the color of the solution again turned reddish-brown. With time, a gradual blue shift to the lower wavelength was observed, as seen previously. The above results clearly indicate the capability of ceria NPs for catalytic oxidative recovery ($Ce^{3+}$-$Ce^{4+}$-$Ce^{3+}$) thus behaving as an anti-oxidant.

The antioxidant property of the ceria NPs is controlled by the oxygen vacancy level in the nanocrystals. It has been proposed that the antioxidant property of ceria nanoparticles is due to the presence of mixed valence states ($Ce^{3+}$ and $Ce^{4+}$) on the NP surface. During the catalytic process, $Ce^{3+}$ ions are converted to $Ce^{4+}$. The system is regenerated via a series of surface chemical reactions between ions in solution and the $Ce^{4+}$ ions on the nanoparticles surface, where they are converted back to $Ce^{3+}$.

The complete process is depicted in the following reactions as proposed in the literature [**4, 11, 36**]**.**

$$H_2O_2 \rightarrow 2[OH\cdot] \quad (2)$$

$$Ce_2O_3 + 2[OH\cdot] = 2CeO_2 + H_2O \quad (3)$$

$$2CeO_2 + H^+(aq) \rightarrow Ce_2O_3 + \frac{1}{2}O_2 \quad (4)$$

## APPLICATION

Ceria is widely used in the field of optics, electrochemistry, catalysis, oxygen storage, bio application for free radical scavenging and solid oxide fuel cell etc. This unique property of ceria NPs was utilized to prevent radiation induced cellular damage, retinal degeneration etc.

## CONCLUSION

In summary, we have synthesized nearly mono-dispersed, ultra small (3.0 ± 0.5 nm) ceria NPs by simple aqueous solution route at room temperature. In addition, we have also synthesized a series of ceria NPs with different sizes through hydrothermal and solvothermal approaches. Studies reveal the formation of single crystalline ceria NPs with mixed valence state of Ce ions ($Ce^{3+}$ and $Ce^{4+}$). The NPs exhibited autocatalytic behavior as investigated through a $H_2O_2$ test coupled with UV-visible transmission measurements. These studies indicated that the present NPs could be directly used as an anti-oxidant in various biomedical applications.

## REFERENCES

[1]. A. Asati, S. Santra, C. Kaittanis, S. Nath, J. M. Perez, Oxidase-like activity of polymer-coated cerium oxide nanoparticles, *Ang. Chem.-Int. Ed.***2009**, 121, 2344-2348.
[2]. S. Babu, S. Velez, K. Wozniak, J. Szydlowsks, S. Seal, Electron paramagnetic study on radical scavenging properties of ceria nanoparticles, *Chem. Phy. Lett.*, **2007**, 442, 405-408.
[3]. J. Chen, S. Patil, S. Seal, J. F. McGinnis, Rare earth nanoparticles prevent retinal degeneration induced by intracellular peroxides, *Nature Nanotech.*, **2006**, 1, 142-150.
[4]. M. Das, S. Patil, N. Bhargava, J. F. Kang, L. M. Riedel, S. Seal, J. J. Hickman, Auto-catalytic ceria nanoparticles offer neuroprotection to adult rat spinal cord neurons, *Biomaterials*, **2007**, 28, 1918-1925.
[5]. P. Dutta, S. Pal, M. S. Seehra, Y. Shi, E. M. Eyring, R. D. Ernst, Concentration of $Ce^{3+}$ and Oxygen Vacancies in Cerium Oxide Nanoparticles, *Chem. Mater*., **2006**, 18 (21), 5144-5146.
[6]. K. Eguchi, T. Setoguchi, T. Inoue, H. Arai, Electrical properties of ceria-b ased oxides and their application to solid oxide fuel cells, *Sol. St. Ionics*,**1992**, 52, 165-172.
[7]. X. Feng, D. C. Sayle, Z. L. Wang, M. S. Paras, B. Santora, A. C. Sutorik, T. X. T. Sayle, Y. Yang, Y. Ding, X. D. Wang, Y. S. Her, Converting Ceria Polyhedral Nanoparticles into Single-Crystal Nanospheres, *Science*, **2006**, 312, 1504-1508.
[8]. Q. Fu, H. Saltsburg, M. Flytzani-Stephanopoulos, Active Nonmetallic Au and Pt Species on Ceria-Based Water-Gas Shift Catalysts, *Science*, **2003**, 301, 935-938.
[9]. T. Hibino, A. Hashimoto, T. Inoue, J. I. Tokuno, S.I. Yoshida, M. Sano, A Low-Operating-Temperature Solid Oxide Fuel Cell in Hydrocarbon-Air Mixtures, *Science*, **2000**, 288, 2031-2033.
[10]. N. Izu, W. Shin, N. Murayama, Fast response of resistive-type oxygen gas sensors based on nano-sized ceria powder, *Sens. Act. B: Chem.*, **2003**, 93, 449-453.
[11]. S. Kar, C. Patel, S. Santra, Direct Room Temperature Synthesis of Valence State Engineered Ultra-Small Ceria Nanoparticles: Investigation on the Role of Ethylenediamine as a Capping Agent, *J.Phys. Chem. C*, **2009,** 113 (12), 4862-4867.
[12]. J. Kaspar, P. Fornasiero, Nanostructured materials for advanced automotive de-pollution catalysts, *J. Sol. St. Chem.*, **2003,** 171, 19-29.
[13]. C. Laberty-Robert, J. W. Long, E. M. Lucas, K. A. Pettigrew, R. M. Stroud, M. S. Doescher, D. R. Rolison,Sol−Gel-Derived Ceria Nanoarchitectures: Synthesis, Characterization, and Electrical Properties, *Chem. Mater*., **2006**, 18(1), 50-58.
[14]. S. Patil, S. C. Kuiry, S. Seal, R. Vanfleet, Synthesis of Nanocrystalline Ceria Particles for High Temperature Oxidation Resistant Coating, *J.Nanoparticle Res.*,**2002**, 4, 433-438.
[15]. G. A. Silva, Seeing the benefits of Ceria, *Nature Nanotech*. **2006**, 1, 92-94.

[16]. Z. L. Wang, X. Feng,Polyhedral Shapes of $CeO_2$ Nanoparticles, *J. Phys. Chem*. B, **2003**, 107 (49), 13563-13566.
[17]. F. Zhang, Q. Jin, S-W. Chan,Ceria nanoparticles: Size, size distribution and shape, *J. Appl. Phys.*, **2004**, 95, 4319.
[18]. P. Jasinski, T. Suzuki, H. U. Anderson, Nanocrystalline undoped Ceria oxygen sensor, *Sens. Act. B: Chem.*, **2003**, 95, 73-77.
[19]. J. J. Hickman, M. Das, S. Patil, N. Bhargava, J. F. kang, L. Riedel, S. Seal, Auto-catalytic Ceria nanoparticles offer neuroprotection to adult rat spinal cord neurons, *Tissue Eng.*, **2007**, 13, 873.
[20]. R. W. Tarnuzzer, J. Colon, S. Patil, S. Seal, Vacancy Engineered Ceria Nanostructures for Protection from Radiation-Induced Cellular Damage, *Nano Letters*, **2005**, 5(12), 2573-2577.
[21]. L. Madler, W. J. Stark, S. E. Pratsinis, Flame-made Ceria Nanoparticles, *J. Mater. Res.*, **2002**, 17, 1356-1362.
[22]. H. Oh, S. Kim, Synthesis of Ceria nanoparticles by flame electrospray pyrolysis, *J.Aerosol Sc.*, **2007**, 38, 1185-1196.
[23]. A. S. Deshpande, N. Pinna, P. Beato, M. Aantonietti, N. Niederberger, Synthesis and Characterization of Stable and Crystalline $Ce_{1-x}Zr_xO_2$ Nanoparticle Sols, *Chem. Mater.*, **2004**, 16 (13), 2599-2604.
[24]. M. Inoue, M. Kimura, T. Inui, Transparent colloidal solution of 2 nm ceria particles, *Chem.Commun.*, **1999**, 957**.**
[25]. J. Zhang, S. Ohara, M. Umetsu, T. Naka, Y. Hatakeyama, T. Adschiri,Colloidal Ceria Nanocrystals: A Tailor-Made Crystal Morphology in Supercritical Water, *Adv. Mater.*, **2007**, 19, 203-206.
[26]. T. Masui, K. Fujiwara, K. I. Machida, G. Y. Adachi, Characterization of Cerium(IV) Oxide Ultrafine Particles Prepared Using Reversed Micelles, *Chem. Mater.*,**1997**, 9 (10), 2197-2204.
[27]. H. Wang, J. J. Zhu, J. Zhu, X. H. Liao, S. Xu, T. Ding, H. Y. Chen, Preparation of nanocrystalline ceria particles by sonochemical and microwave assisted heating methods, *Phys. Chem. Chem. Phys.*, **2002,** 4, 3794-3799.
[28]. T. Yu, J. Joo, I. Y. Park, T. Hyeon, Large-Scale Nonhydrolytic Sol–Gel Synthesis of Uniform-Sized Ceria Nanocrystals with Spherical, Wire, and Tadpole Shapes, *Angew. Chem.-Int. Ed.*, **2005**, 44, 7411.
[29]. J. Maji, S. Basu, K. Maji, Synthesis of Copper Sulphide Nanoparticle By Using Capping Agent CTAB, *J. Applicable Chem.*, **2015**, 4(3), 1007-1011.
[30]. G. Mamidi, S. Polaki, Synthesis and Characterization of Biogenic Silver Nanoparticles and its Antimicrobial Analysis, *J. Applicable Chem.*, **2019**, 8(1), 112-123.
[31]. V. Prakash, R. K. Diwan, U. K. Niyogi, Synthesis and Characterization of Copper Oxide Nanopowders And Their Nanofluids, *J. Applicable Chem.*, **2014**, 3(3), 1025-1030.
[32]. R. Gupta, Y. Madan, E. Menghani, Microwave assisted ZnO Nanocatalysed biginelli Synthesis of Pyrazolopyrimidione Derivatives and Evaluation of Their Bioactivity, *J. Applicable Chem.*, **2014**, 3(5) 1955-1966.
[33]. S. Biswas, S. Kar,Fabrication of ZnS nanoparticles and nanorods with cubic and hexagonal crystal structures: a simple solvothermal approach, *Nanotechnology*, **2008**, 19, 045710 (1-11).
[34]. S. Das, S. Kar, S. Chaudhuri,Optical properties of $SnO_2$ nanoparticles and nanorods synthesized by solvothermal process, *J. Appl. Phys.*,**2006**, 99, 114303 (1-7).
[35]. S. Deshpande, S. Patil, S. Kuchibhatla, S. Seal, Size dependency variation in lattice parameter and valency states in nanocrystalline cerium oxide, *Appl.Phys. Lett.*, **2005**, 87, 133113.
[36]. J. M. Perez, A. Asati, S. Nath, C Kaittanis, Synthesis of biocompatible dextran-coated nanoceria with pH-dependent antioxidant properties, *Small*, **2008**, 4, 552.